

and G. L. Salinger, *Bull. Amer. Phys. Soc.* **19**, 257 (1974).

<sup>5</sup>J. Holder, A. V. Granato, and L. E. Rehn, *Phys. Rev. Lett.* **32**, 1954 (1974); L. E. Rehn, J. Holder,

A. V. Granato, R. R. Coltman, and F. W. Young, Jr., *Phys. Rev. B* **10**, 349, 363 (1974).

<sup>6</sup>P. Erhart and W. Schilling, *Phys. Rev. B* **8**, 2604 (1973).

## Nonlocal Effects in Photoemission Studies with Nonnormally Incident Light

K. L. Kliewer

*Ames Laboratory—USAEC and Department of Physics, Iowa State University, Ames, Iowa 50010*

(Received 24 June 1974)

The local theory for the photoyield resulting from  $p$ -polarized light incident upon a half-space photoemitter is reviewed and generalized to include nonlocal effects. Local and nonlocal yields for the electron gas are presented for frequencies above the plasma frequency. The nonlocal yields are substantially higher than the corresponding local yields and it is shown that this enhancement involves nondirect electronic transitions associated with both plasmons and single-particle excitations.

Optical experiments are usually analyzed by characterizing the material under investigation by a local dielectric function  $\epsilon(\omega) = \epsilon_1(\omega) + i\epsilon_2(\omega)$ . That such a characterization is incomplete for metals is indicated by a nonlocal optical theory<sup>1,2</sup> in which longitudinal excitations, not included in a local description, result from  $p$ -polarized incident light. In most investigations of these nonlocal effects, the only longitudinal excitation included has been the plasmon. The single-particle excitations have also been included in those studies in which the author has participated.

A theory for the photoelectric yield based upon the local dielectric representation has been given by Pepper<sup>3</sup> and Endriz and Spicer.<sup>4</sup> Although the nonlocal effects mentioned above do not strongly modify the local optical properties for a thick sample when realistic values for the mean electron lifetime are included, this need not be true in the case of photoemission since the nonlocal effects are concentrated near the surface<sup>5</sup> and the electron escape lengths are short.<sup>6</sup> In this note the local photoemission theory is summarized and then generalized to the nonlocal realm for the electron gas using the nonlocal theory of Fuchs and Kliewer.

Consider  $p$ -polarized light of frequency  $\omega$  incident from vacuum at an angle  $\theta$  from the normal upon a half-space photoemitter described by a local dielectric function. The reflectance  $R_p$  for

this system is  $R_p = |(\cos\theta - Z_p)/(\cos\theta + Z_p)|^2$ , with  $Z_p$ , the local surface impedance, given by  $Z_p = (\epsilon - \sin^2\theta)^{1/2}/\epsilon$ , and the absorptance  $A_p$  is  $A_p(\theta, \omega) = 1 - R_p$ . With  $z$  increasing into the photoemitter whose surface is the plane  $z = 0$ , the absorbed energy is distributed according to  $(dA/dz) = \alpha A_p \exp(-\alpha z)$ , where the absorption coefficient  $\alpha = (2\omega/c) \text{Im}(\epsilon - \sin^2\theta)^{1/2}$  so that  $A_p = \int_0^\infty (dA/dz) dz$ .

If we then assume that the energy absorption processes result in individual electron excitation, the distribution of excited electrons produced within  $dz$  at  $z$  per incident photon is  $(dA/dz) dz$ . By writing the probability that an electron excited at  $z$  will reach the surface as  $\exp(-z/\xi)/2$ , the number of excited electrons reaching the surface per incident photon will be  $n_s = \int_0^\infty dA \times \exp(-z/\xi)/2$ . The quantity  $\xi$ , which we call the electron escape depth, is a function of the final-state energy  $E_e$  occurring in the electron excitation process. However, we take it here to be a mean escape length for electrons excited by photons of frequency  $\omega$ , so that  $n_s = A_p [\alpha\xi/(1 + \alpha\xi)]/2$  and the photoyield  $Y_T(\theta, \omega)$  can be written

$$Y_T(\theta, \omega) = n_s \sum_{E_e} F(E_e),$$

where  $F$  is a function describing the probability of escape of excited electrons which reach the surface. We are concerned here with the function which we will refer to as the yield, defined by

$$Y(\theta, \omega) = Y_T(\theta, \omega) / \sum_{E_e} \{F(E_e)/2\} = A_p \alpha \xi / (1 + \alpha \xi). \quad (1)$$

An alternative expression for  $Y$  can be obtained as follows. The time-averaged power absorbed per

unit volume at  $z$  is  $\text{Re}[\vec{J}(z) \cdot \vec{E}(z)^*/2]$ , with  $\vec{E}(z)$  the electric field in the photoemitter and  $\vec{J}(z)$  the current density resulting from  $\vec{E}$ . Dividing by the time-averaged incident energy flux  $(c/8\pi) \cos \theta$  (the electric field incident from vacuum has magnitude unity) yields  $dA/dz$ . Thus,

$$Y = (4\pi/c \cos \theta) \int_0^\infty \text{Re}[\vec{J} \cdot \vec{E}^*] \exp[-z/\xi] dz. \quad (2)$$

Expressions (1) and (2) are identical in the local description.

We now turn to the nonlocal theory and consider the photoemitter to be the half-space introduced above, but now an electron gas for which the surface electron scattering is specular and which, therefore, can be characterized by the nonlocal longitudinal and transverse dielectric functions  $\epsilon_l(\vec{q}, \omega)$  and  $\epsilon_t(\vec{q}, \omega)$ . To afford a direct local-nonlocal comparison, we determine the nonlocal yield using Eq. (2).<sup>7</sup> The nonlocal  $\vec{E}$  and  $\vec{J}$  are obtained using the procedure of Sec. III of Ref. 2. With  $p$ -polarized light incident in the  $x$ - $z$  plane, we find

$$\frac{E_x(z)}{H_y(0)} = \frac{2i\omega}{\pi c} \int_0^\infty dq_z \frac{\cos(q_z z)}{q^2} \left( \frac{q_x^2}{(\omega^2/c^2)\epsilon_t} + \frac{q_z^2}{(\omega^2/c^2)\epsilon_t - q^2} \right), \quad (3a)$$

$$\frac{E_z(z)}{H_y(0)} = \frac{2\omega q_x}{\pi c} \int_0^\infty dq_z \frac{q_z \sin(q_z z)}{q^2} \left( \frac{1}{(\omega^2/c^2)\epsilon_t - q^2} - \frac{1}{(\omega^2/c^2)\epsilon_t} \right); \quad (3b)$$

the  $x$  component of the incident photon wave vector is  $q_x = \omega \sin \theta / c$  and  $q^2 = q_x^2 + q_z^2$ . The factor  $\exp[i(q_x x - \omega t)]$  is understood here and in the current-density components, given by

$$\frac{J_x(z)}{H_y(0)} = \frac{\omega^2}{z\pi^2 c} \int_0^\infty dq_z \frac{\cos(q_z z)}{q^2} \left( \frac{q_x^2(\epsilon_t - 1)}{(\omega^2/c^2)\epsilon_t} + \frac{q_z^2(\epsilon_t - 1)}{(\omega^2/c^2)\epsilon_t - q^2} \right), \quad (4a)$$

$$\frac{J_z(z)}{H_y(0)} = \frac{i\omega^2 q_x}{2\pi^2 c} \int_0^\infty dq_z \frac{q_z \sin(q_z z)}{q^2} \left( \frac{(\epsilon_t - 1)}{(\omega^2/c^2)\epsilon_t} - \frac{(\epsilon_t - 1)}{(\omega^2/c^2)\epsilon_t - q^2} \right). \quad (4b)$$

The magnetic field at the surface,  $H_y(0)$ , can be rewritten in terms of the nonlocal surface impedance  $Z_{p,\text{NL}} = E_x(0)/H_y(0)$ , given by (3a), as  $H_y(0) = 1 + r$ , with  $r = (\cos \theta - Z_{p,\text{NL}})/(\cos \theta + Z_{p,\text{NL}})$ .

We use for  $\epsilon_t(\vec{q}, \omega)$  the self-consistent field dielectric function of Mermin,<sup>8</sup> which includes damping via an effective electron lifetime  $\tau$ . The damping is characterized by the parameter  $\gamma = (\omega_p \tau)^{-1}$ , with  $\omega_p$  the plasma frequency. Since we consider here frequencies above the plasma frequency, the transverse dielectric function can be replaced by  $\epsilon(\omega)$ , its value in the local limit<sup>5</sup>:

$$\epsilon(\omega) = \lim_{\vec{q} \rightarrow 0} \epsilon_t(\vec{q}, \omega) = \lim_{\vec{q} \rightarrow 0} \epsilon_l(\vec{q}, \omega) = 1 - [\Omega(\Omega + i\gamma)]^{-1}, \quad (5)$$

with  $\Omega = \omega/\omega_p$ . We use (5) for the local yield calculations.

In Fig. 1 is shown the yield, as a function of the angle of incidence of the light, for  $\Omega = 1.414$ ,  $\gamma = 10^{-3}$ , and several escape lengths, including  $\xi = \infty$  for which the yield is just the absorptance. In the nonlocal calculation the electron density of sodium was used so that  $\hbar\omega_p = 6.07$  eV and the Fermi velocity  $v_F = 1.07 \times 10^8$  cm/sec. The shape of the local-yield curves has been discussed by Arakawa, Hamm, and Williams.<sup>9</sup>

Turning now to the nonlocal results, we see that, while the shape of the curves is rather like that of the local curves, the magnitudes are much larger. This is true for all  $\Omega > 1$ . The explanation for these strongly enhanced nonlocal yields emerges from Fig. 2 where the absorptance per unit length  $dA/dz$  is plotted as a function of distance in the photoemitter for the sodium density,  $\gamma = 10^{-3}$ , and  $\Omega = 1.155$ , 1.414, and

2.924, with the associated angles those for which the yields are approximately maximal. We see that  $dA/dz$  has large oscillations<sup>10</sup> with a frequency-dependent wavelength. These oscillations are longitudinal in character and their origin can be readily traced. In the nonlocal  $A_p$  and  $dA/dz$ ,  $\epsilon_t$  manifests itself roughly via the energy-loss function  $\text{Im}(-1/\epsilon_t)$ ; so we look to phenomena producing peaks in this function as the source of the dominant longitudinal effects. For  $\Omega = 1.155$ ,  $\gamma = 10^{-3}$ , and the sodium density, the plasmon peak occurs at  $q = 0.570 \text{ \AA}^{-1}$  or  $\lambda = 11.0 \text{ \AA}$ , the wavelength of  $dA/dz$  in Fig. 2. Thus, the oscillation for  $\Omega = 1.155$  is essentially a standing plasmon wave. The same is true for  $\Omega = 1.414$  where the plasmon peak in  $\text{Im}(-1/\epsilon_t)$  occurs at  $q = 0.828 \text{ \AA}^{-1}$  or  $\lambda = 7.59 \text{ \AA}$ . We are now, however, very near the frequency for which the plasmon dispersion curve enters the single-particle excitation region

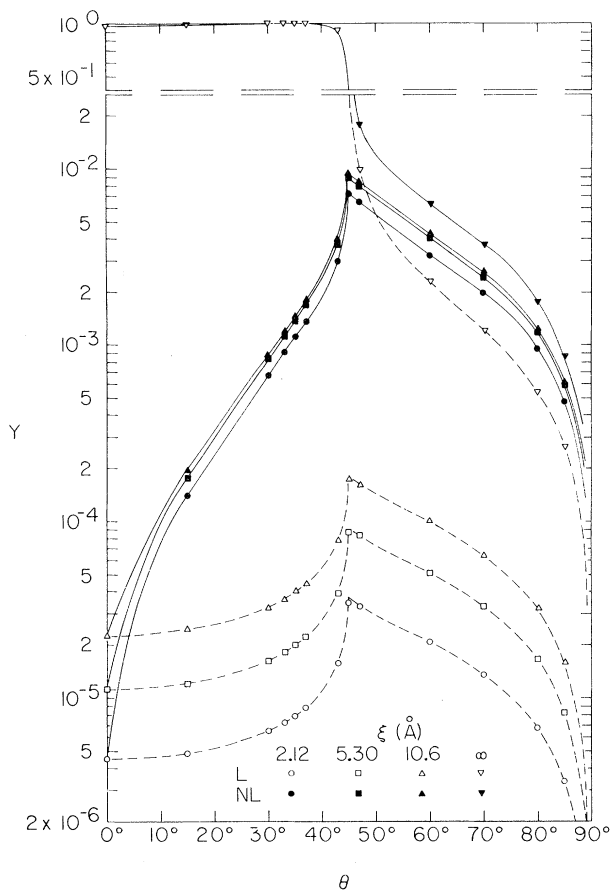


FIG. 1. Local and nonlocal yields for several electron escape depths  $\xi$  versus the angle of incidence of the light for  $\Omega=1.414$ ,  $\gamma=10^{-3}$ , and, nonlocally, the sodium electron density.

with attendant Landau damping; this occurs for the present conditions at  $\Omega \equiv \Omega_L = 1.48$  and  $q \equiv q_L = 0.868 \text{ \AA}^{-1}$ . The plasmon for  $\Omega = 1.414$  is more strongly damped than for  $\Omega = 1.155$ . This together with the proximity of the single-particle region means that the contribution to  $\text{Im}(-1/\epsilon_1)$  from this region is no longer negligible. This is indicated in Fig. 2 by the fact that the wavelength of the oscillations for small  $z$  is somewhat less than the plasmon wavelength.

No significant changes occur in the curves analogous to those of Fig. 1 because of the onset of Landau damping. However, the character of the oscillations in  $dA/dz$  does change. In the frequency region of Landau damping, the plasmon peak in  $\text{Im}(-1/\epsilon_1)$  becomes broad and is superimposed upon the even broader structure in this function resulting from the single-particle excitations.<sup>11</sup> It now is important to recognize that the energy-loss function appears in the theory

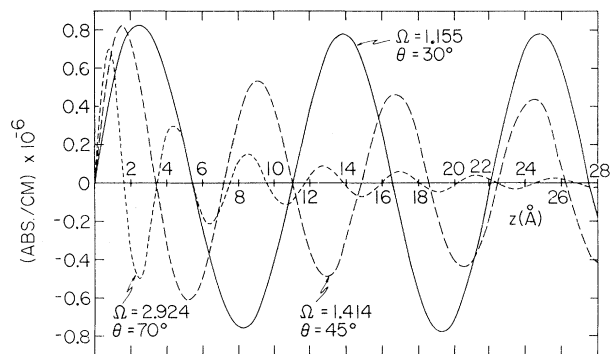


FIG. 2. Nonlocal  $dA/dz$  versus distance for  $\gamma=10^{-3}$  and the sodium electron density.

roughly in the form  $\text{Im}(-1/\epsilon_1)/q^2$ . With Landau damping the  $q$  values of the single-particle excitation region are large, and this function, for fixed  $\Omega$ , will be strongly peaked at a  $q$  value only slightly larger than that of the low- $q$  edge of the single-particle excitation region, the edge described by  $\omega = qv_F + \hbar q^2/2m$ , with  $m$  the electron mass. When  $\Omega = 2.924$ , the low- $q$  edge occurs at  $q = 1.42 \text{ \AA}^{-1}$  or  $\lambda = 4.41 \text{ \AA}$ . It is apparent in Fig. 2 that this value of  $\lambda$  well characterizes the oscillation. The fact that the peak in the function  $\text{Im}(-1/\epsilon_1)/q^2$  includes a small range of wave vectors above that of the edge is indicated in Fig. 2 by the reduced wavelength of the oscillation near  $z=0$  and also by the fact that the oscillations now persist to shorter distances compared with those in the frequency region of the sharp plasmon peaks in  $\text{Im}(-1/\epsilon_1)$ . Thus, both types of longitudinal excitation, plasmons as well as single-particle excitations, contribute strongly to the yield; which dominates depends upon the frequency. We emphasize that these longitudinal effects, associated, as they are, with large wave vectors, involve nondirect electronic transitions.

The  $\gamma$  used above was chosen to be small to emphasize the nonlocal effects. When describing real systems using the electron-gas picture,  $\gamma$  is often taken to be frequency dependent, thereby providing a rough representation of interband effects, and  $\gamma$  may be considerably larger than  $10^{-3}$ . It should be noted, however, that the nonlocal yields can be significantly higher than the local even for  $\gamma \sim 1$ .

In the above calculation of the yield, the basic assumption was that the optical absorption process resulted in excited electrons which could migrate to the surface and escape. However, for

frequencies  $1 < \Omega < \Omega_L$  the nonlocal effects are largely due to the excitation of plasmons; these collective effects can manifest themselves in the yield only to the extent that they decay into single-particle excitations. This process cannot occur in the genuinely free electron gas until  $\Omega > \Omega_L$ ; for a real system plasmon decay can occur at all frequencies due to interband transitions. The inclusion of damping in  $\epsilon_i$  in the present free-electron picture simulates these decay processes as is indicated by a finite plasmon linewidth which increases roughly like  $q^2$  along the plasmon dispersion curve.<sup>11</sup> Because the yield for  $1 < \Omega < \Omega_L$  and  $\theta \neq 0$  is limited by these plasmon-decay processes, we conclude that the above nonlocal theory overestimates, to some extent, the yield to be expected experimentally in this frequency range for materials with long plasmon lifetimes, e.g., aluminum and sodium, but because of nondirect interband transitions as well as the finite plasmon lifetime, the yield will still exceed significantly that of the local description. The overestimate will be largest for  $\Omega \cong 1$ , will decrease with increasing  $\Omega$  as the plasmon lifetime decreases, and will no longer occur for  $\Omega \gtrsim \Omega_L$  as the dominant longitudinal excitations are then of single-particle character.

Although the theory in the present form is for the total yield and does not provide a description of the energy or angular distribution of the excited electrons, one interesting prediction concerning these characteristics does emerge. In the frequency region of Landau damping,  $\Omega \gtrsim \Omega_L$ , it was noted above that the dominant longitudinal effects arise from single-particle excitations occurring near the low- $q$  edge of the single-particle excitation region. This low- $q$  edge corresponds to excitations from an initial state  $\vec{k}$  lying on the Fermi surface with the exciting wave vector  $\vec{q}$  parallel to  $\vec{k}$ . Since the large wave vectors associated with the longitudinal effects are directed essentially normal to the surface [see Eqs. (3) and (4)], the electrons excited are moving normal to the surface. So, for  $\Omega \gtrsim \Omega_L$  and all  $\theta \neq 0$ , the nonlocal enhancement of the yield should appear essentially as electrons from near the Fermi surface leaving the photoemitter approximately normal to the surface.

The present theory is macroscopic in character, based as it is upon  $\epsilon(\vec{q}, \omega)$ . That is, only the diagonal elements of the dielectric tensor have been retained and local-field corrections are not included. As is clear from Fig. 2, the scale of spatial variation for  $\Omega \gtrsim 3$  is such that this may no longer be valid.

Additional questions arise as to the validity of the specular scattering model and the role of surface roughness. Experiments on low-absorption materials such as sodium ( $\hbar\omega_p \cong 5.7$  eV), aluminum ( $\hbar\omega_p \cong 15.0$  eV), and silicon ( $\hbar\omega_p \cong 16.6$  eV) would be helpful in answering these questions.

<sup>1</sup>V. P. Silin and E. P. Fetisov, Zh. Eksp. Teor. Fiz. 41, 159 (1961) [Sov. Phys. JETP 14, 115 (1962)]; A. M. Fedorchenko, Zh. Tekh. Fiz. 32, 589 (1962), and 36, 1327 (1966) [Sov. Phys. Tech. Phys. 7, 428 (1962), and 11, 992 (1967)]; F. Sauter, Z. Phys. 203, 488 (1967); F. Forstmann, Z. Phys. 203, 495 (1967); A. R. Melnyk and M. J. Harrison, Phys. Rev. Lett. 21, 85 (1968), and Phys. Rev. B 2, 835, 851 (1970); W. E. Jones, R. Fuchs, and K. L. Kliewer, Phys. Rev. 178, 1201 (1969); R. Fuchs and K. L. Kliewer, Phys. Rev. 185, 905 (1969).

<sup>2</sup>K. L. Kliewer and R. Fuchs, Phys. Rev. 172, 607 (1968).

<sup>3</sup>S. V. Pepper, J. Opt. Soc. Amer. 60, 805 (1970).

<sup>4</sup>J. G. Endriz and W. E. Spicer, Phys. Rev. B 4, 4159 (1971).

<sup>5</sup>A. J. Mansure, Ph.D. thesis, Iowa State University, 1971 (unpublished).

<sup>6</sup>C. J. Powell, to be published; C. R. Brundle, J. Vac. Sci. Technol. 11, 212 (1974); J. C. Shelton, to be published.

<sup>7</sup>In this way, electron escape is treated the same in the two cases. A preferable procedure would be to do the nonlocal calculation, including the treatment of escape, quantum mechanically using the  $\vec{A} \cdot \vec{p} + \vec{p} \cdot \vec{A}$  interaction, with the nonlocal effects incorporated into the vector potential  $\vec{A}$ .

<sup>8</sup>N. D. Mermin, Phys. Rev. B 1, 2362 (1970).

<sup>9</sup>E. T. Arakawa, R. N. Hamm, and M. W. Williams, J. Opt. Soc. Amer. 63, 1131 (1973).

<sup>10</sup>For  $\Omega = 1.414$ ,  $\theta = 45^\circ$ , and  $\gamma = 10^{-3}$ ,  $dA/dz = 1.64 \times 10^2$  cm<sup>-1</sup> at  $z = 0$  locally.

<sup>11</sup>K. L. Kliewer and H. Raether, Phys. Rev. Lett. 30, 971 (1973), and J. Phys. C: Proc. Phys. Soc., London 7, 689 (1974).